ADC common noise correction and zero suppression in the PIBETA detector

E. Frlež [a,1], D. Počanić [a], S. Ritt [a,b]

[a] *Department of Physics, University of Virginia, Charlottesville, VA 22904-4714, USA*

[b] *Paul Scherrer Institut, Villigen PSI, CH-5232, Switzerland*

We describe a simple procedure for reducing ADC common noise in modular detectors that does not require additional hardware. A method using detector noise groups should work well for modular particle detectors like segmented electromagnetic calorimeters, plastic scintillator hodoscopes, cathode strip wire chambers, segmented active targets, and the like. We demonstrate what we call "second pedestal noise correction" method by comparing representative ADC pedestal spectra for various elements of the PIBETA detector before and after the applied correction.

PACS Numbers: 07.50.H, 07.05.Hd, 07.05.Kf

Keywords: ADC pedestals, correlated common noise, DAQ zero suppression

[1] Corresponding author; Tel: +1–804–924–6786, fax: +1–804–924–4576, e–mail: frlez@virginia. edu (E. Frlež)

1 Introduction

Experimental areas in particle accelerator facilities are notoriously noisy places due to beamline elements like magnets, slits, pumps, power supplies, and ventilators as well as other assorted electronics equipment that runs continuously or is intermittently turning on and off. That causes voltage ripples that significantly compromise photomultiplier tube (PMT) current pulses digitized by analog-to-digital converters (ADCs). The problem is compounded especially in analysis of data from segmented detectors where total energies or directions of measured particles are derived from smeared ADC values of several adjacent detector modules. An experimenter might try to follow the recipes for reduction of pedestal noise couplings by designing recommended magnetic shielding and applying proper electrical grounding principles [1–3]. But such efforts are in practice usually met with only limited success.

In order to minimize the electronic noise arising from dirty electrical grounds and a cross-talk between adjacent detector ADC channels quality coaxial cables should be used for connecting PMT anode outputs with inputs of fast electronics units. This arrangement though does not protect against stray magnetic fields at low frequencies that cause so-called "ground loops".

While a low frequency noise contribution could be easily removed by using isolation transformers and capacitor-coupled inputs to the ADCs, that approach is not an option in high-rate environments where AC-coupled devices would produce unacceptable signal distortions and rate-dependent baseline shifts.

Custom electronic circuits developed to address the problem of low frequency voltage ripples are described in Refs. [4,5]. They were designed to provide a correspondence between a simple saw-tooth waveform and an experimental AC-power cycle, locking that information and passing it to data stream for an offline noise correction.

Another method that uses one or more "blackened PMTs" (bPMTs) in parallel with the detector active PMTs is described and compared with active AC-noise synchronization circuits in Ref. [5]. The bPMTs are dummy phototubes under high voltage but with no attached detector modules whose signals are digitized in exactly the same way as those of the active detectors. A drawback/disadvantage of the method is that for complicated experimental layouts operating in noisy environments and with multiple local grounds prevailing in the areas close to the beamlines more than a handful of the bPMTs would be necessary to properly account for the correlated noise. Moreover, because bPMTs should be mechanically and electrically a part of a detector and should be physically close the active PMTs, they could be affected by, for example, Cherenkov radiation caused by relativistic minimum ionizing particles in pho-

tocathode glass windows, destroying the noise correlations.

In the analysis that follows we take advantage of a fact that our apparatus consists of individual detectors that are optically isolated from each other. Therefore, one particular physics trigger will not excite more than a handful of active detectors and a role of a "blackened PMT" could be played by different active detector lines in different events. We call our procedure "the second pedestal noise correction".

2 Experimental layout

The PIBETA apparatus [6] is a large acceptance 3π sr nonmagnetic detector optimized for measurements of electrons and photons in energy range of 10–100 MeV. The heart of the detector is a spherical 240-module pure CsI calorimeter that is supplemented with a segmented 9-piece active plastic target, a pair of conventional cylindrical MWPCs, and a cylindrical 20-counter plastic hodoscope for charged particle tracking and identification.

All parts of the detector are mounted at the center of a 2.5×5.6 m steel platform that also carries high voltage supplies, a detector cooling system, coiled coaxial delay cables on the one side and fast trigger electronics on the opposite side of the platform. Therefore, the PIBETA detector is a compact self-contained assembly that can be moved easily from its parking place into a chosen experimental area as a single unit and made operational within a day. Due to the detector proximity to elements of a beamline our fast electronics was exposed to a significant contaminating electronic hum. Fig. 1 shows a typical baseline of an analog signal that was to be digitized in an ADC device. The signal is captured on a Tektronix TDS 744 digital oscilloscope. A snapshot displays ground loops noise with frequencies of $\sim$50 Hz and $\sim$300 Hz in a 20 μs interval. A typical noise amplitude was $\leq$5 mV.

PMT signal outputs were split either directly at the PMT voltage dividers or at passive custom-made analog signal splitters. One branch of the analog signal was delayed $\sim$250 ns in coaxial cables and then split again to provide inputs for FASTBUS ADC units and discriminators/TDCs/scalers. The other branch of the PMT signal was connected to discriminator or summer modules of the fast trigger electronics. The master trigger outputs were delayed and subsequently used to provide ADC gates and TDC start/stop signals. Metal frames of the PMT high voltage supplies on one end of the platform and the detector conductive support structure in the center were connected with 10 mm/20 mm thick copper cables to fast trigger electronics grounding points in order to decrease the noise arising from the ground loops. Voltage differences

between different parts of the detector were measured with a digital voltmeter and after the grounding connections were in place were reduced to less then 4 mV.

For digitizing fast PMT pulses we have used a LeCroy ADC model 1882F unit, a high-density FASTBUS converter with 96 current-integrating negative inputs [7]. The 1885F unit provided a wide dynamic range with 12-bit data for the resolution of 0.05 pC/count and less than 1 % quantization error. Raw pedestals were set at about channels 200-300 and in our particular experimental environment had the average root-mean-square (rms) widths of ≈15-20 channels.

Fig. 2 presents an analog signal of a single CsI calorimeter detector on 2 mV/division and 100 ns/division scale taken in 6 sec persistence mode. Clearly, with an ADC gate width set to 100 ns, the ADC unit will integrate variable amounts of the noise current. A 70 MeV electron or photon will produce the current pulse with an amplitude of ∼0.25 V and a ∼30 ns FWHM width. This current pulse into 50 Ω will integrate to a charge of about 150 pF, placing it at 3/4 of a full scale. A common noise with an amplitude 5 mV present on the baseline will integrate in a 100 ns gate to a 10 pF charge, or almost 7% of an actual particle signal. As the energies and/or directions of measured particles are deduced from ADCs of a centrally hit calorimeter module and up to seven of its nearest neighbors, the resulting uncertainty in energy (direction) could add up to 20%.

3 Random (Pedestal) Trigger

A $190 \times 20 \times 8\,\mathrm{mm}^3$ plastic scintillator counter (BC-400) was placed horizontally above the electronics racks, about 3 m away from the main PIBETA detector. By a virtue of its position, the counter was shielded from the experimental radiation area by a 5 cm thick lead brick wall as well as by a 50 cm wide concrete wall. Operating with a high discriminator threshold it was counting only random cosmic muons at about 1-2 Hz frequency, having a stable counting rate for both beam-on and beam-off periods.

The discriminated signals from that scintillator counter defined our random trigger. The main PIBETA detector trigger was defined dynamically in a programmable logic unit. In practice, the master trigger was a logic OR of up to 12 individual triggers. High rate physics triggers in the mix were prescaled, with prescaling factors depending on the trigger type and the beam stopping rate. The random trigger was connected to the trigger mix logic unit and in production runs it was always included among the enabled triggers. A single

production run was limited to 200,000 events, yielding typically $\sim 10^4$ random triggers per run interspaced among the physics triggers.

We note parenthetically that in an off-line analysis ADC values for all detectors in random events were written out to a text file. These data sets were used in a `GEANT` [8] detector simulation, enabling us to rigorously account for the residual ADC noise and accidental event pile-ups in energy spectra.

4 Common Noise Groups

In a pre-production calibration run data were first collected in so-called "pedestal mode" with the beam off and with only random trigger enabled in the trigger mix. Raw pedestals were automatically calculated at the end of the calibration run. Namely, the pedestal histograms were filled with the random trigger events R_{ni} expressed in ADC channel numbers, where a subscript n labels a detector and an index i represents an event number. At the end of the run these histograms were analyzed for the mean pedestal positions P_n. The mean pedestal positions and widths were saved in an online database residing completely in shared memory to allow for fast access. "Calibrated ADC values" C_i in the subsequent production runs would then be differences between raw ADC readings R_{ni} and the pedestal values P_n retrieved from the online database:

$$C_{ni} = R_{ni} - P_n. \tag{1}$$

The analyzer calibration program also calculated the correlation coefficients r_{nm} among all possible detector pairs "nm" that belong to the same detector group, e.g., for 240 calorimeter detectors, 40 plastic veto hodoscope counters, etc. The expression used for calculating the correlation coefficient r_{nm} was [9]:

$$r_{nm} = \frac{N\sum_{i=1}^{N} C_{ni}C_{mi} - \sum_{i=1}^{N} C_{ni}\sum_{i=1}^{N} C_{mi}}{\sqrt{N\sum_{i=1}^{N}(C_{ni})^2 - (\sum_{i=1}^{N} C_{ni})^2}\sqrt{N\sum_{i=1}^{N}(C_{mi})^2 - (\sum_{i=1}^{N} C_{mi})^2}}, \tag{2}$$

where sums extend over all pedestal events with ADC values greater than 20 channels and N is the total number of such events.

The correlation coefficient matrix was saved in a text file that was was analyzed by an offline code to identify the detector noise groups. A user of the program could select the maximum number of noise groups (default 10), minimum group size (default 8) and the minimum correlation coefficient (default

0.75) between the detectors in the same noise group. With quoted default parameters we would usually end up with nine scintillator detector noise groups having an average intergroup correlation coefficient $\approx$0.90 and minimum correlation coefficient greater then 0.75.

The noise groups suggested by the program were then hard-wired in the analyzer calibration program. An example of six plastic hodoscope (PV) noise groups is given below in a piece of the `C` code:

```
/* ADC groups for common noise suppression */

#define MAX_NOISE_GROUP 100
int adc_group[][MAX_NOISE_GROUP] = {

  /* Plastic Veto Detectors */

  {240,241,242,243,244,245,246,247,248,
   249,250,251,252,253,254,255, -1},
  {256,257,258,259, -1},
  {260,261,262,263,264, -1},
  {265,266,267,268,269,270,271, -1},
  {272,273,274,275, -1},
  {276,277,278,279, -1},
  { -1 },                          };
```

where individual PV counters are identified by their signal indices. The value "-1" at the end of each line follows the last detector in every noise group. Each detector is included in one and only one noise group. The detectors belonging to the same noise group are usually physically close and have their signal and high voltage cables bundled together.

The algorithm for calculation of the noise-corrected and calibrated ADC values resides in the analyzer program running with predefined noise groups, loops over all ADC channels and for every event:

(i) subtracts the raw pedestal values retrieved from the online database from raw ADC variables;
(ii) identifies the common noise group that the current detector belongs to;
(iii) finds the channel with the smallest ADC value in that group;
(iv) finds all the channels in the group under consideration which are less than 15 counts above the minimum of the group and calculates their average ADC value;
(v) subtracts that average value ("second pedestal correction") from the ADC values of all other group members.

At the beginning of each run the pedestal histograms are now reset and at the end of the run they are again analyzed by fitting lineshapes with the Gaussian function. The means of the distributions are updated in the database as new pedestal values P_n.

5 Results and Discussion

Fig. 3 shows a scatter plot of ADC values for two different CsI detectors acquired with a random trigger. Uncorrected ADC values are plotted in the top panel showing the correlation in an electronic noise: these two detectors were eventually assigned to the same electronics noise group. Using the secondary pedestal correction procedure described above, we obtained a scatter-plot of the corrected ADC values presented in the lower panel of Fig. 3.

Examples of one-dimensional ADC histograms for two different detector types, namely a plastic scintillator counter and one active target segment are shown in Figs. 4 and 5, respectively. Top panels represent raw ADC spectra, bottom panels show the noise suppression in the corrected spectra.

In Fig. 4 a peak at channel number 6 is inserted by a fitting function in the analyzer program. Its position corresponds to 3 standard deviations of the corrected pedestal lineshape. In readout of the ADC modules all channels with the values below 3σ were suppressed by being considered equal to zero and were not written to tape. This zero suppression criterion compressed the size of our data files by an order of magnitude.

A comparison between the smearing of raw pedestal data and the spectra obtained after the noise suppression for four different detector types is given in Table 1. The table summarizes the maximum and minimum noise group sizes, rms widths of raw and corrected pedestal histograms as well as an important equivalent energy deposition corresponding to the corrected pedestal rms values. We see that the energy equivalents of the rms widths range from 0.13 MeV in CsI detectors to 0.40 MeV in the segmented target. The target pedestals are more difficult to correct because of the small number of target segments (9) making a noise group and high rate of physics triggers in the target, with up 1 MHz stopping pions.

6 Conclusion

We have shown how to correct modular detector ADC readings for the correlated common noise using the method of detector common noise groups. The reduction in the pedestal width of up to a factor of five was achieved with the corrected pedestal rms values as narrow as 1.5 ADC channels. This improvement compares favorably with the active circuit noise suppression methods [4,5] where improvements factor were ∼5-6.

In a representative case of pure CsI calorimeter the procedure reduces the correlated noise contribution to the equivalent energy to 0.13 MeV per detector module. For the energy range of interest, 10–100 MeV, this value is smaller than the photoelectron statistics contribution of $\sqrt{E/60}$ MeV [10] and is comparable with the PMT dark current noise that amounts to ∼0.1 MeV.

7 Acknowledgements

This work is supported and made possible by grants from the US National Science Foundation and the Paul Scherrer Institute.

References

[1] H. W. Ott, *Noise Reduction Techniques in Electronics Systems*, (John Wiley, New York, 1976).

[2] P. Horowitz and W. Hill, *The Art of Electronics*, 2nd Ed., Ch. 7 (Cambridge University Press, Cambridge, 1989).

[3] M. Johnson, *Practical Electronics for Experimenters*, Fermilab Academic Lecture Series, (Fermilab, Batavia, 1990).

[4] P. H. Garbincius, *A Simple Analog Clock Used for Reducing Pedestal Noise*, FERMILAB-TM-2049 Preprint, (Fermilab, Batavia, 1996).

[5] W. J. Llope, N. Adams, and K. K. Kainz, *An electronic clock for correlated noise corrections*, Nucl. Instrum. Meth. A443 (2000) 451.

[6] D. Počanić, D. Day, E. Frlež, R. M. Marshall, J. S. McCarthy, R. C. Minehart, K. O. H. Ziock, M. Daum, R. Frosch and D. Renker, PSI R-89.01 Experiment Proposal, (Paul Scherrer Institute, Villigen, 1988).

[7] LeCroy 1995 Research Instrumentation Catalog, (Chestnut Ridge, NY, 1995).

[8] R. Brun, F. Bruyant, M. Maire, A. C. McPherson, and P. Zanarini, `GEANT3`, CERN publication DD/EE/84-1, (CERN, Geneva, 1987).

[9] P. R. Bevington and D. K. Robinson, Data Reduction and Error Analysis for the Physical Sciences, 2nd Ed., (McGraw Hill, New York, 1992).

[10] E. Frlež, Ch. Brönnimann, B. Krause, D. Počanić, D. Renker, S. Ritt, P. L. Slocum, I. Supek, and H. P. Wirtz, e-print hep-ex/0006027.

Fig. 1. A typical low frequency noise in the electronics house next to the πE1 area at Paul Scherrer Institute. The average amplitude of the correlated noise is $\leq$5 mV and the frequency range 50–500 Hz.

Fig. 2. A typical analog signal baseline for a single CsI PIBETA detector. The detector is part of the 240-element PIBETA calorimeter. The baseline oscillation is $\sim$3 mV, which is integrated over a 100 ns ADC gate.

Fig. 3. ADC signal correlation for two CsI detectors making the 240-module PIBETA electromagnetic calorimeter. The trigger is a random event trigger.

Fig. 4. Improvement in the pedestal width for one plastic veto scintillator making up the 40-stave PIBETA hodoscope. Dashed line represents the raw pedestals, the solid line shows the corrected pedestals.

Fig. 5. Improvement in the pedestal width for one channel of the 9-piece segmented active target after the common noise correction.

Table 1
The comparison of the pedestal noise reduction for the various elements of the PIBETA detector. The values represent averages in one typical production run with ∼5000 pedestal events. The minimum and maximum number of detectors in one noise group is given in second column. The energy (angle) equivalent of the corrected pedestal *rms* is listed in the fifth column.

Detector Type (Number)	Group Size Min/Max	Raw Pedestal <rms> (ch)	Corrected Ped. <rms> (ch)	Corr. Ped. En. (Angle) Equivalent
CsI Calorimeter Module (240)	13/48	20.9	3.3	0.13 MeV
Plastic Scintillator Stave (40)	4/16	16.9	2.7	0.01 MeV
Active Plastic Target (9)	9/9	21.1	4.6	0.40 MeV
MWPC Cathode Strip (192/384)	128/384	104	35	0.06°

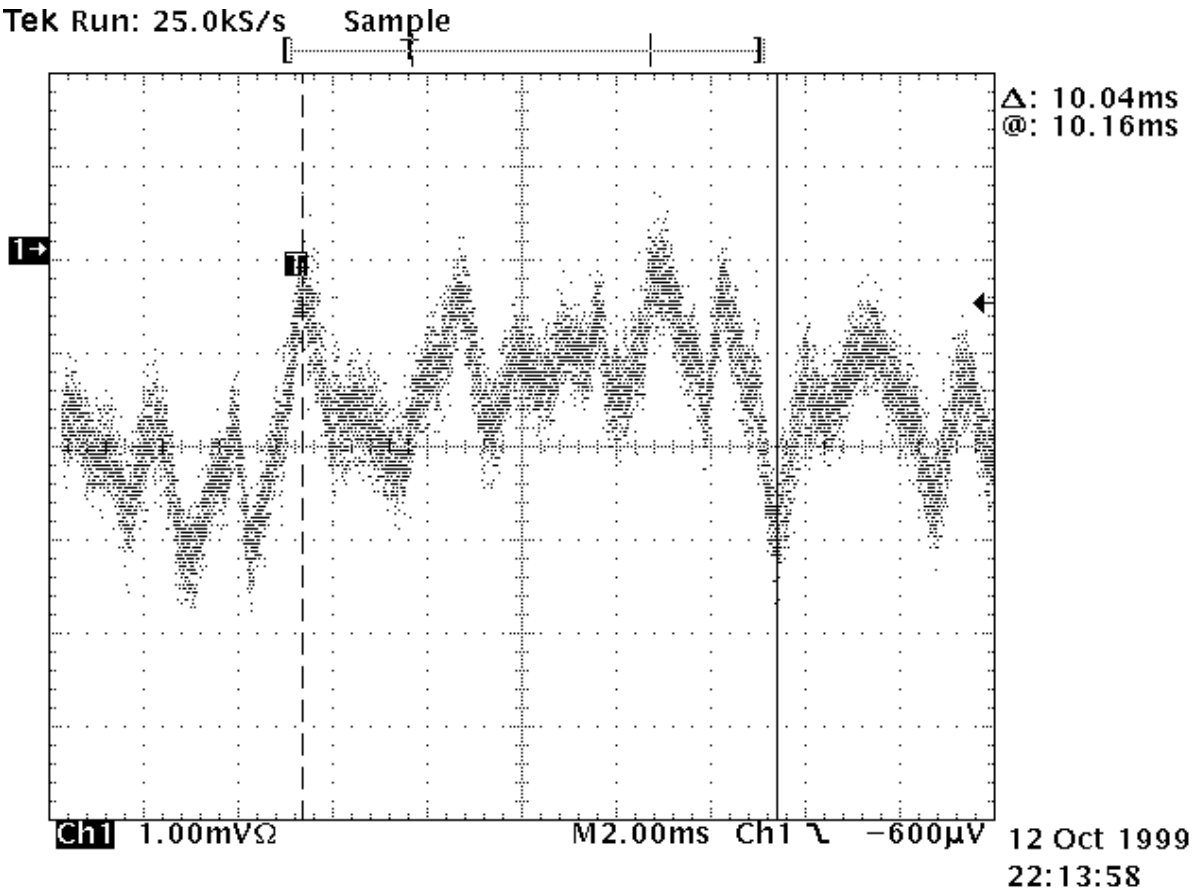
Tek Run: 25.0kS/s Sample
Δ: 10.04ms
@: 10.16ms
Ch1 1.00mVΩ
M2.00ms Ch1 ∖ −600µV
12 Oct 1999
22:13:58

FIGURE 1

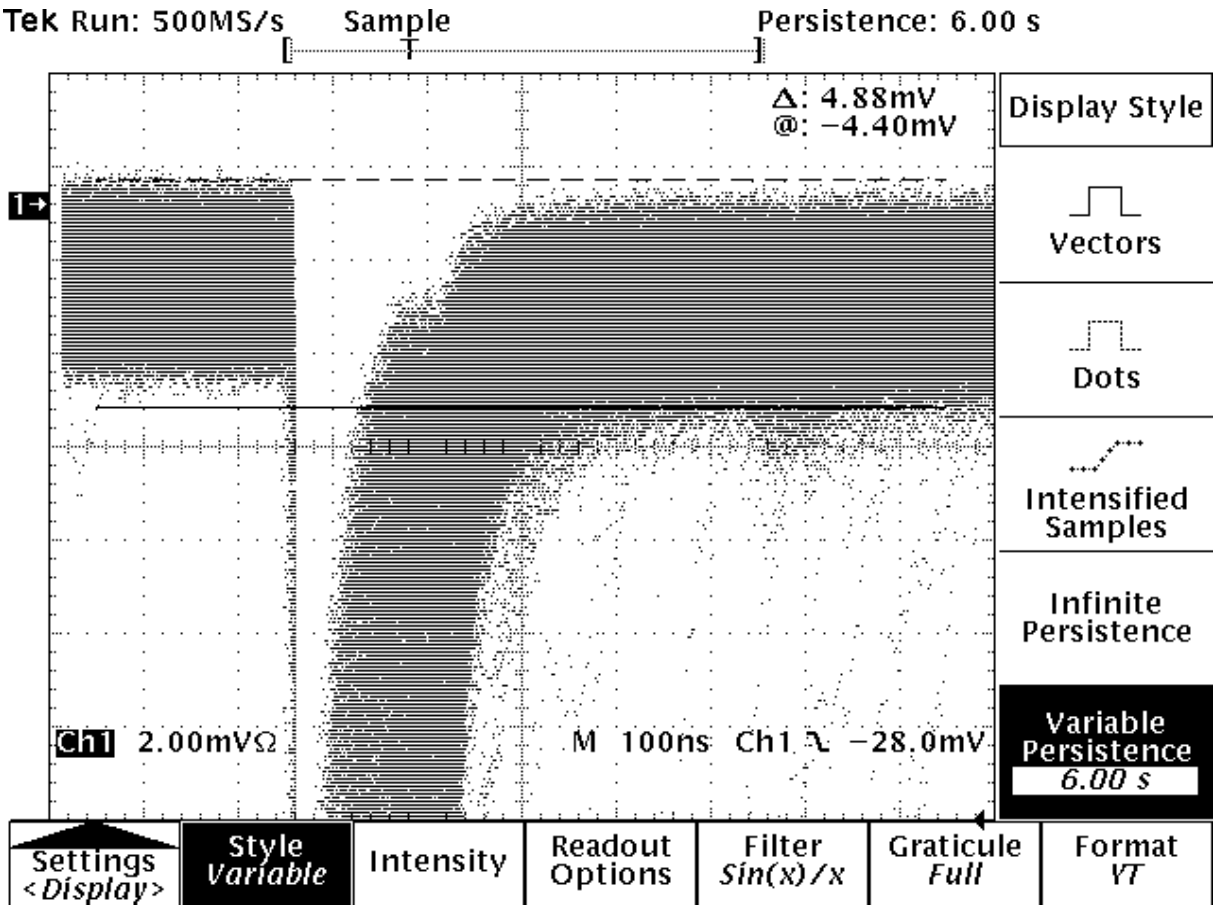
Tek Run: 500MS/s Sample
Persistence: 6.00 s
Δ: 4.88mV
@: −4.40mV
Display Style
Vectors
Dots
Intensified Samples
Infinite Persistence
Variable Persistence
6.00 s
Ch1 2.00mVΩ
M 100ns Ch1 ∿ −28.0mV
Settings <Display>
Style Variable
Intensity
Readout Options
Filter Sin(x)/x
Graticule Full
Format YT

FIGURE 2

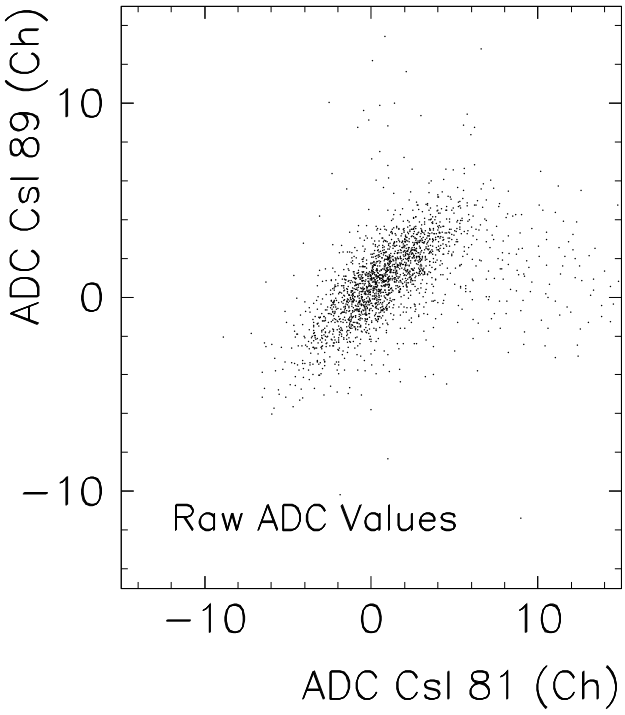
ADC CsI 89 (Ch)
10
0
−10
Raw ADC Values
−10
0
10
ADC CsI 81 (Ch)

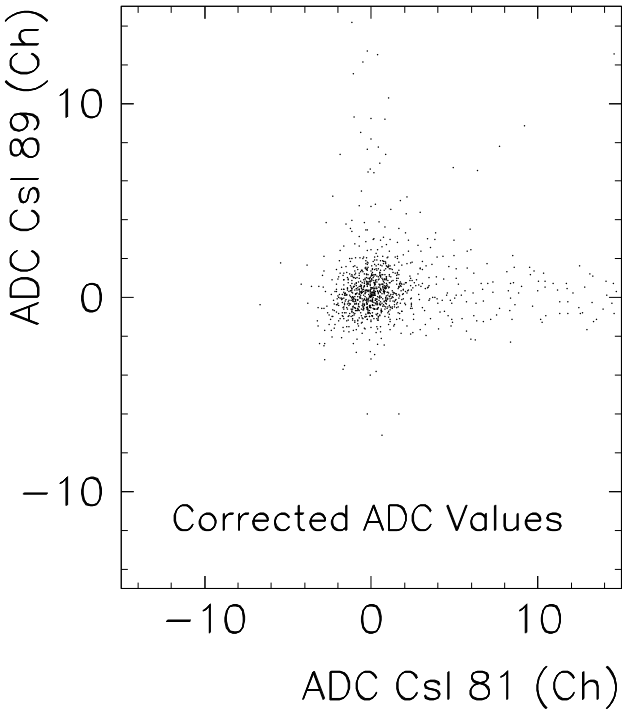
ADC CsI 89 (Ch)
10
0
−10
Corrected ADC Values
−10
0
10
ADC CsI 81 (Ch)

FIGURE 3

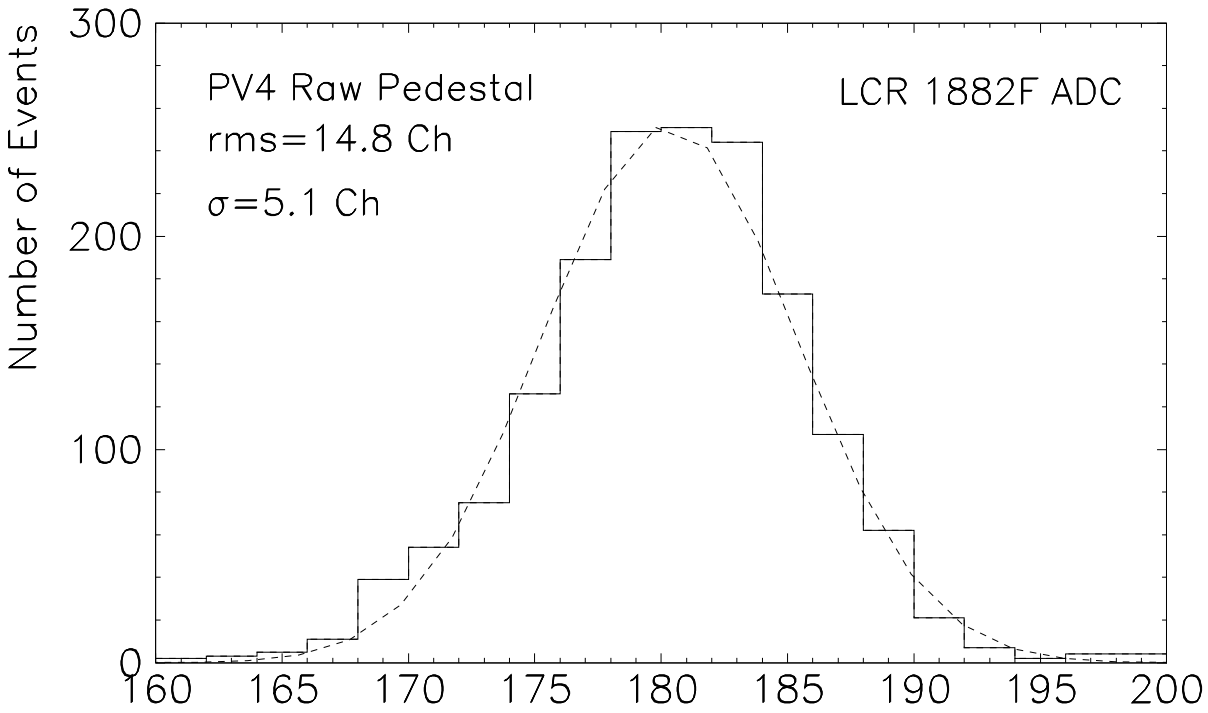
PV4 Raw Pedestal
rms=14.8 Ch
σ=5.1 Ch
LCR 1882F ADC
Number of Events
300
200
100
0
160
165
170
175
180
185
190
195
200

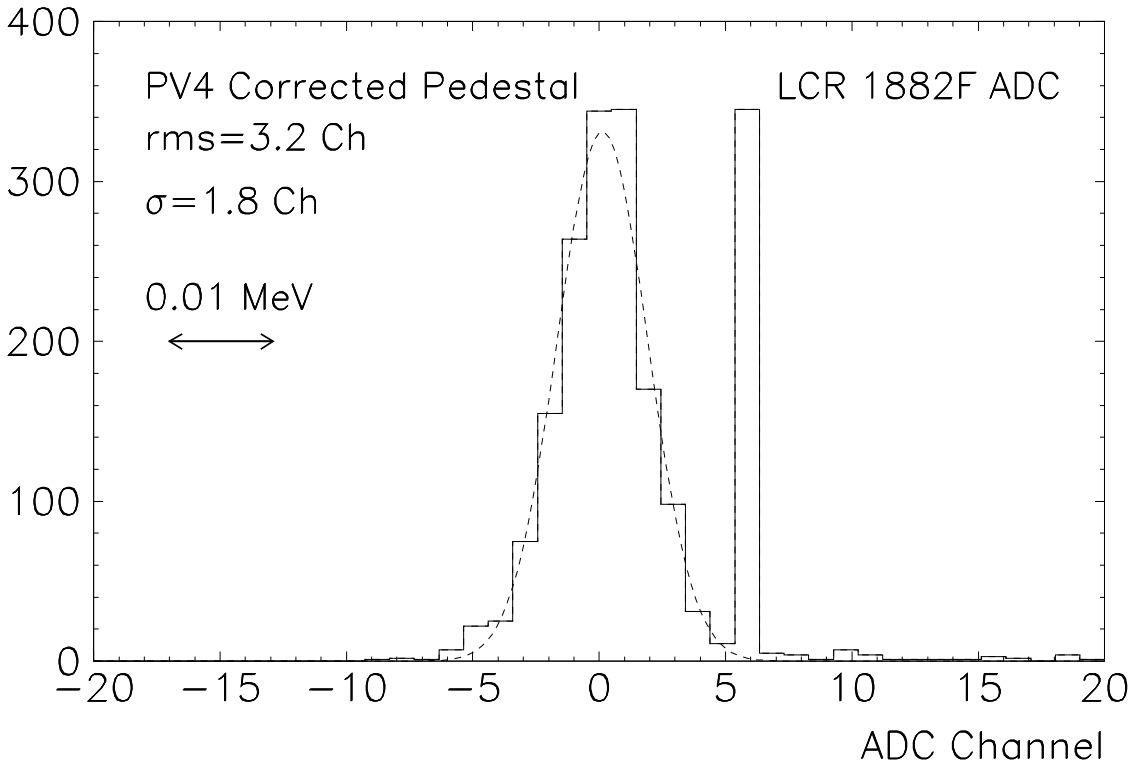
PV4 Corrected Pedestal
rms=3.2 Ch
σ=1.8 Ch
0.01 MeV
LCR 1882F ADC
400
300
200
100
0
−20
−15
−10
−5
0
5
10
15
20
ADC Channel

FIGURE 4

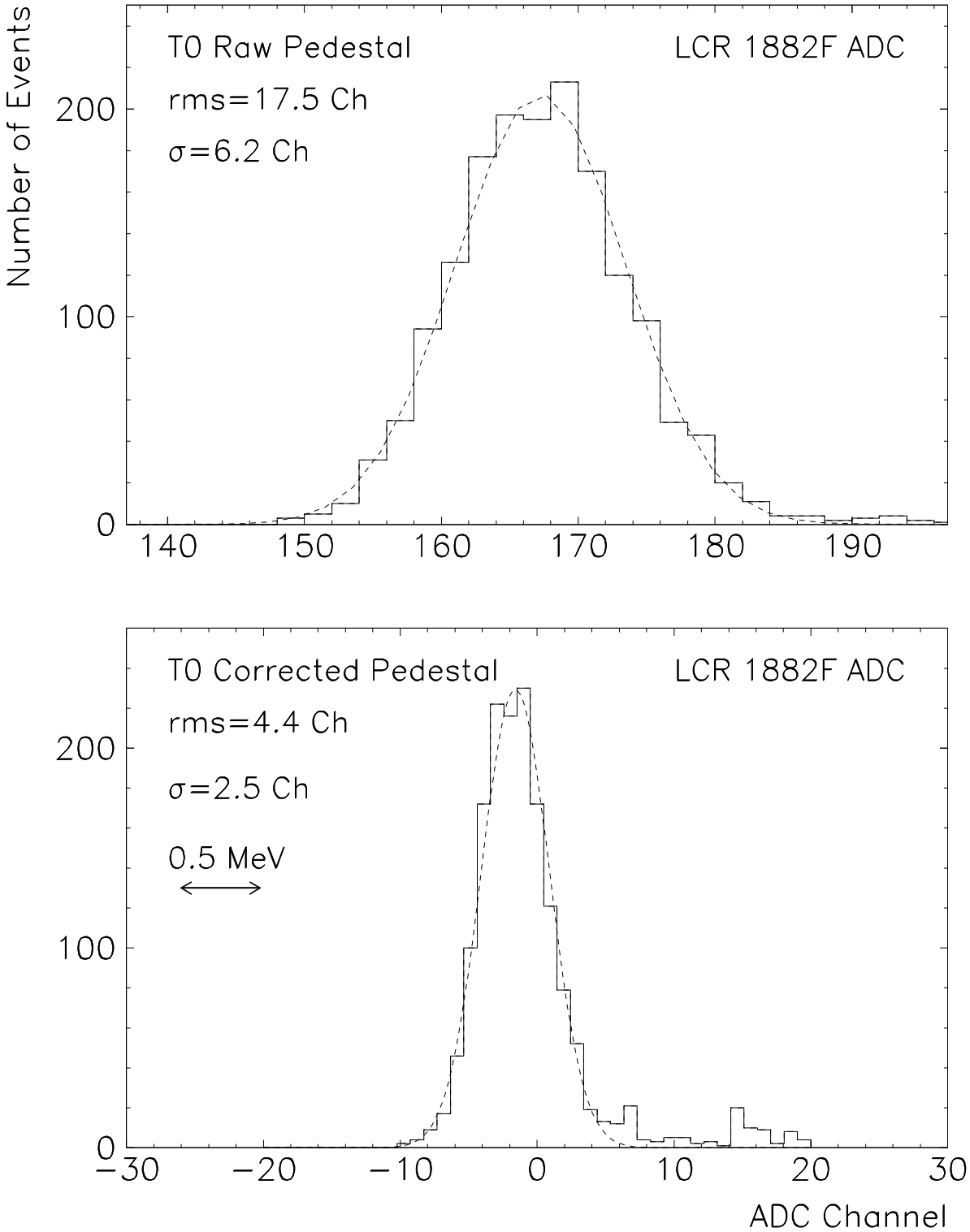
T0 Raw Pedestal
LCR 1882F ADC
rms=17.5 Ch
σ=6.2 Ch
Number of Events
200
100
0
140
150
160
170
180
190
T0 Corrected Pedestal
LCR 1882F ADC
rms=4.4 Ch
σ=2.5 Ch
0.5 MeV
200
100
0
−30
−20
−10
0
10
20
30
ADC Channel

FIGURE 5